2.10 Relationship of Tropical Circulation and Energetics using Retrieved Surface and Atmospheric Radiation Budget (SARB) for January—August 1998

Thomas P. Charlock[1], Fred G. Rose[2], David Rutan[2],
David P. Kratz[1], Zhonghai Jin[2], Lisa H. Coleman[3], and Qiang Fu[4]
[1]NASA Langley Research Center, Atmospheric Sciences Competency, Hampton, VA
[2]Analytical Services and Materials Inc., Hampton, VA
[3]SAIC Inc., Hampton, VA
[4]Department of Atmospheric Sciences, University of Washington, Seattle, WA

Introduction

A complete and accurate description of the Surface and Atmosphere Radiation Budget (SARB) — the vertical profiles of radiative fluxes that drive the general circulation and the hydrological cycle — is one of the fundamental goals of research on physical climate. Almost every GCM computes such profiles. One step on the way has been the computation of the SARB in a limited domain (Charlock and Alberta, 1996) using cloud optical properties retrieved with satellites (Minnis et al., 1995) and carefully selected input data for atmospheric soundings. Here we report a new determinination of the SARB over the tropics for January-August 1998 using the Clouds and the Earth s Radiant Energy System (CERES) top of the atmosphere (TOA) record (Wielicki et al., 1996) on the Tropical Rainfall Measurement Mission (TRMM) satellite. The approach has been to compute the SARB with a radiative transfer code and partly constrain (tune) both the outputs and inputs using CERES. The results so far have been useful mainly in a diagnostic sense, permitting a series of elaborate cross checks among radiative transfer theory, satellite and sounding inputs, and alternate methods for computing the forcing due to clouds, aerosols, humidity, and surface albedo. We provide below an abbreviated summary of the retrieveal algorithm; a comparison of computed and observed fluxes; and an illustration of the relationship of one of the profiles that we produce to the atmospheric circulation.

Retrieval of Flux Profiles

The CERES SARB is the product of the Fu and Liou (1993) radiative transfer code, which has been highly modified (Rose and Charlock, 2002). The most critical inputs for this application of the code are the cloud optical properties (fractional area, optical depth, particle size, height of top, and estimate of geometrical thickness). Cloud retrievals (Minnis et al., 2002) using small (~ 1km) VIRS imager pixels are matched to each of the large (~20km) CERES footprints. Other inputs include temperature and humidity from ECMWF (Rabier et al., 1998), SBUV and TOVS ozone profiles (Yang et al., 2001), aerosol optical thickness (AOT) from an assimilation that employs AVHRR and NCEP (Collins et al., 2001) or alternately from VIRS (Stowe et al., 1997), and assigned aerosol optical properties (Hess et al., 1998).

The radiation code is run at least twice for each broadband CERES footprint, in order to adjust inputs that determine the vertical profile of radiative fluxes. Constrainment (Rose et al. 1997; Charlock et al. 1997) is an approach to minimize the normalized, least squares differences between (1) computed TOA fluxes and adjusted values for key inputs and (2) observed TOA fluxes and initial values for key inputs. The algorithm assigns an a priori numerical sigma (uncertainty) to each TOA flux and key input parameter. For clear sky footprints over the ocean, the constrainment adjusts the surface skin temperature, lower tropospheric humidity (LTH), upper tropospheric humidity (UTH), and AOD using CERES TOA observations of LW broadband irradiance and radiance, 8.1-11.8 micron window (WN) filtered radiance, and SW irradiance. For clear footprints over land, the surface albedo is also adjusted; and the sigma (a priori uncertainty) for skin temperature is increased, causing a larger adjustment in skin temperature over land than over ocean. We do not adjust air temperature above the surface. For cloudy or partly cloudy footprints, the parameters below TOA used to constrain clear footprints are frozen; cloud optical depth, cloud fractional area, and cloud top height are adjusted instead. Cloud optical depth is modified by adjusting liquid water path or ice water path, rather than droplet or crystal size.

CERES observations at TOA are obviously regarded as more accurate than either tuned or untuned calculations. The constrainment (or tuning) algorithm does NOT yield a perfect match to CERES at TOA. For March, April, and May of 1998, the tuned calculations for reflected SW at TOA are further from the CERES observations than the untuned calculations (Fig. 1). Note that the untuned LW at TOA (OLR) is a few Wm-2 larger than the CERES observations, and the untuned reflected SW flux is generally smaller than CERES. Over roughly 40N-40S during this 8 month period, there is an increasing tendency for CERES to both emit more in the thermal IR and to reflect more in the SW, than we see in the untuned calculations; this is the case for clear skies, too (not shown), for which the effect of the VIRS imager on the radiative transfer inputs is minimal.

Corresponding Author:
Thomas P. Charlock
Mail Stop 420
NASA Langley Research Center
Hampton, VA 23681 (t.p.charlock@larc.nasa.gov)

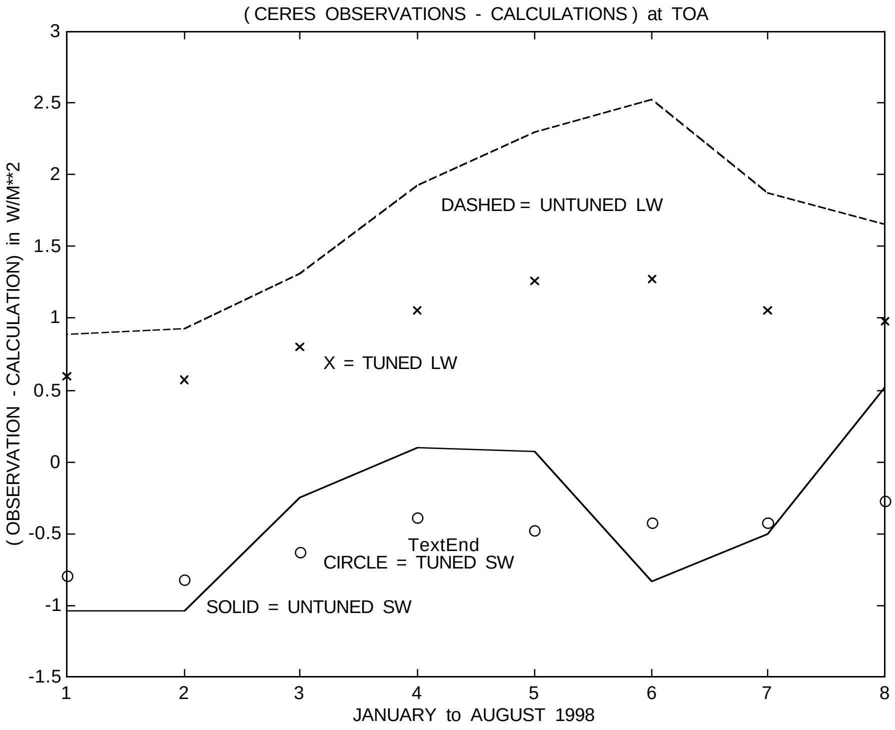

Figure 1. Difference of CERES observations and calculations for TRMM domain (~40S-40N) during January-August 1998; as a simple, ungridded mean from an enormous number of footprint scale differences. Untuned calculations with Fu-Liou code using ECMWF data and cloud properties from VIRS imager. Tuned calculations use adjusted inputs.

Table 1 compares tuned results at one site with observations. The constrainment (tuning) does NOT use ground-based data; the surface radiometers are here a cold test. The most significant discrepancies are for daylight mean suface insolation and surface albedo in both clear and cloudy conditions. We suspect that the ground-based surface albedo measurements, which are from short towers over designated yards, are not representative of larger areas. The retrieved insolation would be a better match to observations if the code had slightly more gaseous absorption (some parameters are based on a compilation from 1982) or if a higher fraction of soot were assigned to the specified AOT. Ground-based photometers indeed measured larger values of AOT than were used in the calculations. For the full set of valiation sites available on line (Rutan et al. 2001)
http://www-cave.larc.nasa.gov/cave/
the bias in retrieved insolation is larger (-31 Wm-2 for all sky) than at the ARM Central Facility. The SW bias in Table 1 is expressed as daytime mean; 24-hour biases would be smaller by a factor of 2.

	Obs Mean	N	Bias Obs-Tuned
ALL SKY	Wm-2		Wm-2
LW Dn Sfc	352	448	1
LW Up Sfc	421	423	2
SW Dn Sfc	431	258	-18
SW Up Sfc	85	258	9
LW Up TOA	248	454	0
SW Up TOA	224	258	2
CLEAR SKY			
SW Dn Sfc	516	94	-19

Table 1. Bias of tuned fluxes at ARM Central Facility. Observations (Obs) of surface (Sfc) fluxes, down (Dn) and up, at site E13 for January-August 1998. TOA observations from CERES**.**

Example of Radiation/Circulation Relationship

The SARB product includes LW/SW/WN fluxes (up and down) at the surface, 500 hPa, 200 hPa, 70 hPa, and TOA. Sample results follow.

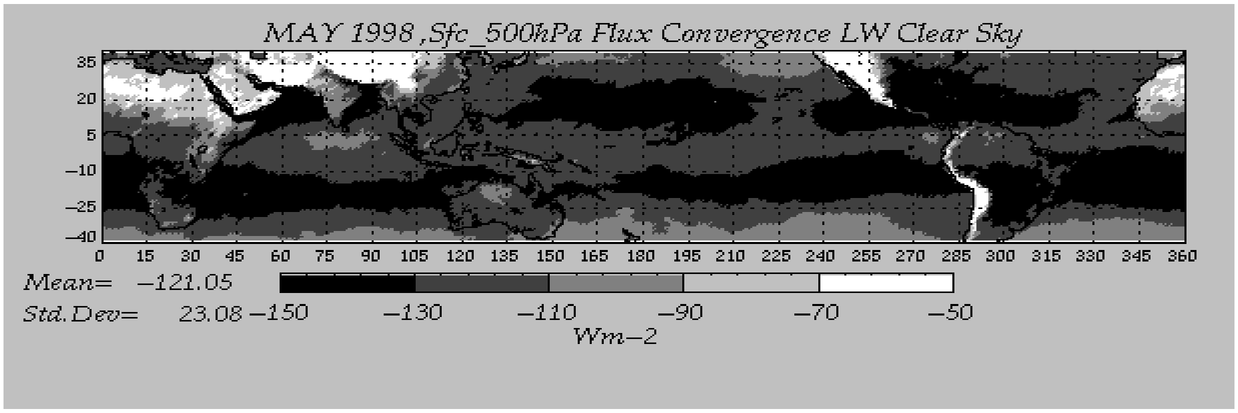

Figure 2. Retrieved convergence of LW in clear skies between surface and 500 hPa, as rough mean (not diurnally smoothed) for May 1998. We define radiative convergence as the difference of net fluxes for the top and bottom of the specified layer. In the darkest regions above, clear sky LW cooling in the lower troposphere counters the warming associated with adiabatic subsidence in the subtropical branches of the Hadley cell.

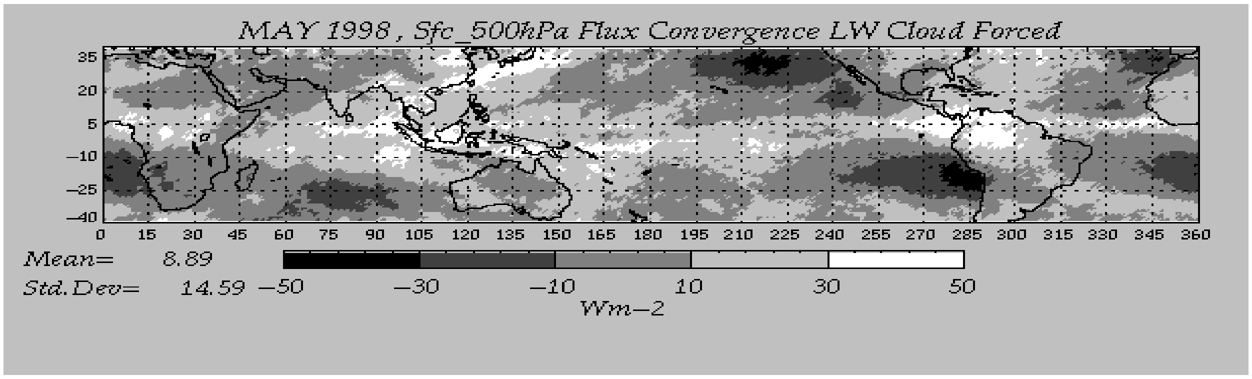

Figure 3. Cloud forcing to retrieved convergence of LW between surface and 500 hPa, as rough mean (not diurnally smoothed) for May 1998. The ~100 Wm-2 algebraic span of cloud forcing (here from -50 to +50 Wm-2) is as large as the clear sky cooling in Figure 2 (-50 to -150 Wm-2). Light colored areas above show regions where clouds (often above the 500 hPa level) tend to suppress LW cooling of the lower troposphere. In the marine stratocumulus zones, cloud forcing reverses sign and enhances clear sky LW cooling, thereby supporting large scale subsidence.

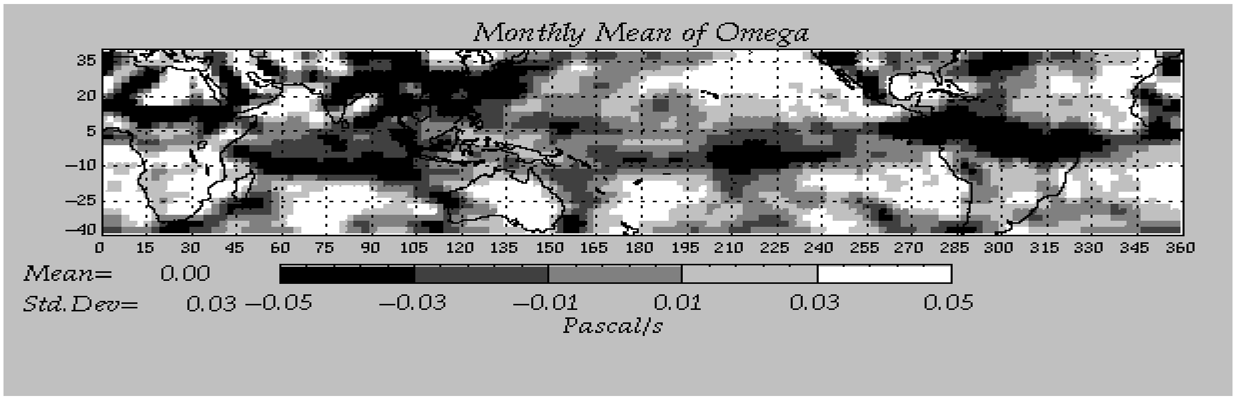

Figure 4. Omega (dp/dt) at 700 hPa (NCEP Reanalysis, May 1998). Dark denotes ascent at 700 hPa, here representing the middle of the surface-to-500 hPa layer of Figures 2 and 3. The lightest zones over the oceans have descending air, where stratocumulus (dark regions in Figure 3) radiative effects facilitate the dynamics.

A higher quality, color version of this document is available from
http://www-cave.larc.nasa.gov/cave
under Publications . The same URL has validation data on line, sample results, etc.

References

Charlock, T. P., and T. L. Alberta, 1996: The CERES/ARM/GEWEX Experiment (CAGEX) for the retrieval of radiative fluxes with satellite data. Bull. Amer. Meteor. Soc., 77, 2673-2683.

Charlock, T. P., F. G. Rose, D. A. Rutan, T. L. Alberta, D. P. Kratz, L.H. Coleman, G. L. Smith, N. Manalo-Smith, and T. D. Bess, 1997: Compute Surface and Atmospheric Fluxes (System 5.0), CERES Algorithm Theoretical Basis Document. 84 pp. See http://asd-www.larc.nasa.gov/ATBD/.

Collins, W. D., P. J. Rasch, B. E. Eaton, B. V. Khattatov, J.-F. Lamarque, and C. S. Zender, 2001: Simulating aerosols using a chemical transport model with assilimiation of satellite aerosol retrievals: Methodology for INDOEX. J. Geophys. Res., 106, 7313-7336.

Fu, Q., and K.-N. Liou, 1993: Parameterization of the radiative properties of cirrus clouds. J. Atmos. Sci., 50, 2008-2025.

Hess, M., P. Koepke, and I. Schult, 1998: Optical Properties of Aerosols and Clouds: The software package OPAC. Bull. Amer. Meteor. Soc., 79, 831-844

Minnis, P., W. L. Smith, Jr., D. P. Garber, J. K. Ayers, and D. R. Doelling, 1995: Cloud properties derived from GOES-7 for spring 1994 ARM Intensive Observing Period using Version 1.0.0 of ARM satellite data analysis program. NASA Reference Publication 1366, 58 pp.

Minnis, P., D. F. Young, B. A. Wielicki, D. P. Kratz, P. W. Heck, S. Sun-Mack, Q. Z. Trepte, Y. Chen, S. L. Gibson, and R. R. Brown: 2002: Seasonal and Diurnal Variations of Cloud Properties Derived from VIRS and MODIS Data. 11th Conference on Atmospheric Radiation (AMS), 3-7 June 2002 in Ogden, Utah.

Rabier, F., J.-N. Thepaut, and P. Courtier, 1998: Extended assimilation and forecast experiments with a four-dimensional variational assimilation. Quart. J. Roy. Meteor. Soc., 124, 1861-1887.

Rose, F. G., and T. P. Charlock, 2002: New Fu-Liou Code Tested with ARM Raman Lidar and CERES in pre-CALIPSO Exercise. 11th Conference on Atmospheric Radiation (AMS), 3-7 June 2002 in Ogden, Utah.

Rose, F., T. Charlock, D. Rutan, and G. L. Smith, 1997: Tests of a constrainment algorithm for the surface and atmospheric radiation budget. Proceedings of the Ninth Conference on Atmospheric Radiation, Long Beach (Feb. 2-7, 1997), AMS, 466-469.

Rutan, D. A., F. G. Rose, N. Smith, and T. P. Charlock, 2001: Validation Data Set for CERES Surface and Atmospheric Radiation Budget (SARB). GEWEX News, Vol. 11, No. 1 (February), pp. 11-12. Available at www.gewex.com under Newsletter .

Stowe, L. L., A. M. Ignatov, and R. R. Singh, 1997: Development, validation, and potential enhancements to the second generation operational aerosol product at the National Environmental Satellite, Data, and Information Service of the National and Oceanic Atmospheric Administration. J. Geophys. Res., 102, 16,923-16,934.

Wielicki, B. A., B. R. Barkstrom, E. F. Harrison, R. B. Lee, G. L. Smith, and J. E. Cooper, 1996: Clouds and the Earth s Radiant Energy System (CERES): An Earth Observing System Experiment. Bull. Amer. Meteor. Soc., 77, 853-868.

Yang, S.-K., S. Zhou, and A. J. Miller, 2000: SMOBA: A 3-dimensional daily ozone analysis using SBUV/2 and TOVS measurements. URL www.cpc. ncep.gov/ products/stratosphere/SMOBA/smoba_doc.htm